Journal of Solid State Chemistry 187 (2012) 15–19

Contents lists available at SciVerse ScienceDirect

Journal of Solid State Chemistry

journal homepage: www.elsevier.com/locate/jssc

Synthesis, structure, and optical properties of BiCuO*Ch* (*Ch*=S, Se, and Te)

A.P. Richard [a], J.A. Russell [b], A. Zakutayev [b], L.N. Zakharov [a], D.A. Keszler [a], J. Tate [b,*]

[a] Department of Chemistry, Oregon State University, 153 Gilbert Hall, Corvallis, OR 97331-4003, USA
[b] Department of Physics, Oregon State University, 301 Weniger Hall, Corvallis, OR 97331-6507, USA

ARTICLE INFO

Article history:
Received 24 August 2011
Received in revised form
30 October 2011
Accepted 6 November 2011
Available online 4 December 2011

Keywords:
BiCuOSe
Oxychalcogenide
Crystal structure
Band gap
Optical absorption
Solid solution

ABSTRACT

Crystals of BiCuOSe were grown from a salt flux, and the crystal structure was determined by single-crystal X-ray diffraction. BiCuOSe adopts the tetragonal layered structure of *Ln*CuO*Ch* (*Ln*=lanthanide; *Ch*=S, Se, and Te) with bond lengths and bond angles in good agreement with those published for powders. Powders comprising mixed chalcogenides across the series BiCuO*Ch* (*Ch*=S, Se, and Te) were made by reacting Bi_2O_2Ch and Cu_2Ch. Band gaps determined via infrared diffuse reflectance from powders are E_g=0.82 eV for BiCuOSe, 0.89 eV for $BiCuOS_{0.5}Se_{0.5}$, and 1.07 eV for BiCuOS. The band gap of BiCuOSe inferred from infrared transmission measurements on single crystals is in good agreement with the value obtained from diffuse reflectance from the powder.

1. Introduction

Recent single crystal structural investigations of EuCuOSe [1] and LaCuOS [2] emphasize the potential of Cu-based lanthanide oxide chalcogenides of the form *Ln*CuO*Ch* (*Ln*=lanthanide, and *Ch*=S, Se or Te) as *p*-type transparent conductors with significant conductivities, high carrier concentrations, and band gaps as high as 3 eV [3]. The materials belong to the tetragonal space group P4/*nmm*, with layers of $(Ln_2O_2)^{2+}$ and $(Cu_2Ch_2)^{2-}$ stacked alternately along the *c*-axis. Interest in the Bi analogs of the LaCuO*Ch* system stems from the electronic configuration of Bi. The pseudo-closed $6s^2$ shell of Bi^{3+} may hybridize with the *p*-orbitals of the chalcogenide anion at the valence band maximum, improving the hole mobility; such pseudo-closed shells are features of the *p*-type semiconductors SnO and PbS [3]. The energetic position of the Bi-*p* orbitals, which locate near the conduction band minimum, lower the band gap considerably relative to the LaCuO*Ch*, into the 1-eV range, which makes these materials of interest as solar absorbers or thermoelectrics [4]. The Bi analog also forms at considerably lower temperatures. $BiCu_{1-x}OS$ has been reported to exhibit superconductivity at 6 K [5]. BiCuOS and BiCuOSe powders have been prepared by solid state synthesis [3,6] and by hydrothermal methods [7,8], BiCuOTe powders by solid state synthesis [3], and *c*-axis oriented thin films of BiCuOSe by pulsed laser deposition. Transmission and reflection measurements of the oxide selenide films indicate a band gap of 0.8 eV [9]. Diffuse reflectance measurements of powders by Hiramatsu et al. [3] yield an electronic band gap of 1.1 eV for BiCuOS and 0.8 eV for BiCuOSe. Diffuse reflectance from BiCuOTe indicates no clear band edge, but structure in the FTIR spectra suggests a band gap of 0.4–0.5 eV [3]. Stampler et al. report band gaps of 1.09 eV and 0.75 eV for hydrothermally prepared powders of BiCuOS and BiCuOSe, respectively [8].

In this study, mm-sized crystals of BiCuOSe are precipitated from a salt flux. The optical properties of the crystals are compared to those of the corresponding powder. Powders of BiCuO*Ch* (*Ch*=Se and Te) and the solid solutions $BiCuOS_{0.5}Se_{0.5}$ and $BiCuOSe_{0.5}Te_{0.5}$ are produced using a two-step synthesis technique. BiCuOS powder is also made to complete the series. We report the synthesis, structure, and optical properties of the crystals and the powders.

2. Experiment

2.1. Powder synthesis

BiCuOS powder was made from the precursor Cu_3BiS_3, which was prepared from the elements after the method described by Mizota et al. [10]. Stoichiometric amounts of Bi metal (Strem, 99.999%), Cu (Cerac, 99.5%), and S (Alfa Aesar, 99.8%) were placed in a fused silica tube, which was evacuated to 10^{-6} Torr before it was sealed. The tube was heated to 440 °C at 2.5 °C/min and held for 24 h, then raised to 600 °C at 2.5 °C/min and held for at least

* Corresponding author. Fax: +1 541 737 1683.
E-mail address: tate@physics.oregonstate.edu (J. Tate).

0022-4596/$ - see front matter © 2011 Elsevier Inc. All rights reserved.
doi:10.1016/j.jssc.2011.11.013

11 h. The tube was then quenched in water. The resulting power was ground in acetone and resealed in a second fused quartz tube, which was subsequently evacuated to 10^{-6} Torr. The powder was fired a second time at 600 °C (7 °C/min ramp), held for 24 h, cooled to 525 °C in 43 h (at 2 °C/h), held for 5 h, and finally cooled to room temperature. The resulting Cu_3BiS_3 powder was mixed with Bi_2O_3 (Alpha Aesar, 99.99%) according to

$$Bi_2O_3 + Cu_3BiS_3 \rightarrow 3BiCuOS. \quad (1)$$

The powder mixture was placed in Grafoil® packets, sealed in a fused silica tube evacuated to 10^{-6} Torr and heated to 300 °C at 7 °C/min where it was held for 6 h, heated to 500 °C at 7 °C/min, held for 2 h and then cooled to room temperature. The resulting powder was BiCuOS, as confirmed by X-ray diffraction.

BiCuO*Ch* (*Ch*=Se, Te) and BiCuO$Ch'_{0.5}Ch''_{0.5}$ (*Ch*′, *Ch*″=S, Se, and Te) powders were made via a route involving reactions of Bi_2O_2Ch and Cu_2Ch precursors:

$$Cu_2Ch' + Bi_2O_2Ch'' \rightarrow 2BiCuOCh'_{0.5}Ch''_{0.5}. \quad (2)$$

All powder mixtures were sealed in fused silica tubes evacuated to 10^{-6} Torr. Powders made via the reaction in Eq. (2) include $BiCuOS_{0.5}Se_{0.5}$ (reactants heated to 600 °C for 1 day), BiCuOSe (500 °C for 1 day), $BiCuOSe_{0.5}Te_{0.5}$ (500 °C for 5 days) and BiCuOTe (500 °C for 5 days). Cu_2Ch' precursor powders used were Cu_2S (Alfa Aesar, 99.5%), Cu_2Se (Cerac, 99.5%) or Cu_2Te (Cerac, 99.5%). The Bi_2O_2Ch'' precursors were made from Bi_2O_3 (Alpha Aesar, 99.99%) and $Bi_2Ch''_3$ mixed in the appropriate stoichiometric ratio. For the telluride, Bi_2Te_3 (Cerac, 99.99%) was used, and for the selenide, Bi_2Se_3 was made in-house by heating Bi powder (Strem, 99.999%) and Se powder (Cerac, 99.8%) in a 2:3 M ratio, sealing in an evacuated fused silica tube and heating to 800 °C for 12 h. Bi_2O_2Se was formed by heating the Bi_2O_3 and Bi_2Se_3 to 500 °C for 1 week and Bi_2O_2Te was formed by heating Bi_2O_3 and Bi_2Te_3 to 500 °C for 4 weeks [11]. These reactions are summarized below, and italicized type indicates that reagents were obtained from commercial vendors:

$$2Bi + 3Se \xrightarrow{800\,^{\circ}C,12\,h} Bi_2Se_3 \quad (3)$$

$$Bi_2Se_3 + 2Bi_2O_3 \xrightarrow{500\,^{\circ}C,1\,w} 3Bi_2O_2Se \quad (4)$$

$$Bi_2O_2Se + Cu_2S \xrightarrow{600\,^{\circ}C,1\,d} 2BiCuOS_{0.5}Se_{0.5} \quad (5)$$

$$Bi_2O_2Se + Cu_2Se \xrightarrow{500\,^{\circ}C,1\,d} 2BiCuOSe \quad (6)$$

$$Bi_2Te_3 + 2Bi_2O_3 \xrightarrow{500\,^{\circ}C,\,4\,w} 3Bi_2O_2Te \quad (7)$$

$$Bi_2O_2Te + Cu_2Se \xrightarrow{500\,^{\circ}C,5\,d} 2BiCuOSe_{0.5}Te_{0.5} \quad (8)$$

$$Bi_2O_2Te + Cu_2Te \xrightarrow{500\,^{\circ}C,5\,d} 2BiCuOTe \quad (9)$$

2.2. Crystal growth

Bi_2O_2Se and Cu_2Se precursor powders in a 1:1 M ratio were mixed in a flux of equimolar proportions of KCl:NaCl. The reactant to flux molar ratio was 1:10. The flux and starting materials were loaded into an alumina crucible inside a fused silica tube, which was then sealed under vacuum, $P \sim 10^{-6}$ Torr. The evacuated tube was heated in a furnace at a rate of 200 °C/h to 900 °C, held for 24 h, cooled to 575 °C at 5 °C/h, and then cooled at 200 °C/h to room temperature. The crystals were removed from the crucible by immersing it in boiling distilled water to dissolve the KCl and NaCl. The BiCuOSe crystals were then soaked in 1 M HCl for three days.

2.3. Crystal structure of BiCuOSe

Diffraction data from a single crystal of BiCuOSe were collected at 173 K on a Bruker SMART Apex CCD diffractometer using Mo*K*α radiation (0.71073 Å). Integration was performed using the SAINT-Plus package [12] with an applied SADABS absorption correction [13]. The crystal structure was determined by direct methods and refined with a full-matrix least-squares technique. All atoms were refined with anisotropic thermal parameters and the final refinement converged to $R_1=0.0282$ and $wR_2=0.0733$. All calculations were performed by Bruker SHELXTL package [12]. Crystallographic data and details covering data collection and refinement are listed in Table 1. Final atomic positions and displacement parameters are listed in Table 2. The Crystallographic Information File is available as supplemental data.

2.4. Powder X-ray diffraction

Phase purity of powders was verified by X-ray diffraction using Cu*K*α radiation on a Rigaku Miniflex diffractometer with a monochromator. Powder X-ray diffraction was used for phase identification and lattice parameter determination. The *c*- and *a*-axis lattice parameters were determined from a least-squares fit to the positions of the observed X-ray diffraction peaks using the Le Bail method within the GSAS software package [14].

Table 1
Crystallographic data for BiCuOSe and details of the data collection and structure refinement.

Empirical formula	BiCuOSe
Formula weight (amu)	367.48
Temperature (K)	173(2)
Wavelength (Å)	0.71073
Crystal system	Tetragonal
Space group	*P*4/*nmm*
Unit cell dimensions (Å)	$a=b=3.9193(4)$, $c=8.915(2)$
$\alpha=\beta=\gamma$ (deg.)	90
Volume (Å^3)	136.95(4)
Z	2
Density (calculated, g/cm^{-3})	8.912
Absorption coefficient(mm^{-1})	84.884
F(000)	308
Crystal size(mm)	$0.04 \times 0.02 \times 0.01$
Theta range for collection	2.28–26.93°
Index ranges	$-5 \le h \le 4$, $-4 \le k \le 5$, $-11 \le l \le 11$
Reflections collected	1412
Independent reflections	115[$R_{int}=0.0261$]
Completeness to θ=26.93°	100.00%
Absorption correction	Semi-empirical from equivalents
Max and min transmission	0.4840 and 0.1324
Refinement method	Full-matrix least-squares on F^2
Data/restraints/parameters	115/0/12
Goodness-of-fit on F^2	1.323
*R*indices [$I>2\sigma(I)$]	$R_1=0.0282$, $wR_2=0.0733$
*R*indices(all data)	$R_1=0.0290$, $wR_2=0.0735$
Largest diff. peak and hole	2.313 and −2.480 eÅ^{-3}

Table 2
Atomic coordinates, U_{eq}, and anisotropic displacement (Å^2) parameters for BiCuOSe. U_{eq} is defined as one third of the trace of the orthogonalized U^{ij} tensor.

Atom	*x*	*y*	*z*	U_{eq}	$U^{11}=U^{22}$	U^{33}
Bi	1/4	1/4	0.1404(1)	0.0069(5)	0.0055(5)	0.0096(7)
Cu	−1/4	1/4	1/2	0.0123(8)	0.012(1)	0.012(2)
Se	−1/4	−1/4	0.3239(3)	0.0074(7)	0.0063(9)	0.010(1)
O	−1/4	1/4	0	0.008(4)	0.006(5)	0.012(9)

$U^{12}=U^{13}=U^{23}=0$ for all atoms; U_{eq} is one third of the trace of the orthogonalized U^{ij} tensor.

2.5. Compositional analysis

The composition of the crystals was determined using electron probe microanalysis (EPMA) and a Cameca SX-100 analyzer. A few crystals were mounted on an aluminum puck using epoxy and then coated with ~5 nm of graphite. The atomic ratio of Bi:Cu:O:Se was 1.00:1.02:1.12:1.02.

2.6. Optical measurements

Cleaned BiCuOSe crystals were thinned to ~4 μm for transmission measurements. Crystals were mounted onto an aluminum plate using Crystalbond®. The attached crystal was hand ground on a lapping pad using alumina slurry. The slurry was made by mixing 3-μm alumina powder and distilled water until a thick paste formed. After grinding, the crystals were washed with DI water to remove excess slurry. Room temperature transmission measurements in the range 850–2650 nm were obtained using an Ocean Optics NIR 256–2.5 spectrometer with an InGaAs detector. The crystal was tacked onto a glass slide using a very small amount of Crystalbond and mounted close to a circular aperture of about 1.5 mm diameter. Light was incident along the crystal *c*-axis and traversed the crystal and the glass slide, but not the adhesive.

The room temperature optical absorption of BiCuO*Ch* powders was measured using a Thermo Scientific Antaris II FT-NIR spectrometer (Thermo Fisher) in an integrating sphere configuration with a resolution of 16 cm^{-1}. The band gap was estimated from the absorption using the Kubelka–Munk equation to convert diffuse reflection to α/S, where α and S denote the absorption and scattering coefficients, respectively [15,16]. The band gaps were estimated from the low-energy onset of absorption, defined as the energy at the intersection of the relatively flat low-energy absorption and the extrapolation of the steep rise in absorption.

3. Results and discussion

A photograph of the plate-like BiCuOSe crystals is shown in Fig. 1. They are black in color with highly reflective faces. Their average size is about 1 mm in the lateral direction and approximately 12 μm in thickness.

Detailed structural parameters for BiCuOSe are listed in Table 2, and the bond distances and angles are given in Tables 3 and 4. The refinement was carried out assuming full occupancy of each site by the appropriate atom. Refinement allowing variable occupancy of the Cu site, which might be suggested by the relatively large thermal parameter, was not consistent with a Cu vacancy in this case.

BiCuOSe has fluorite-like layers of $(Bi_2O_2)^{2+}$ alternating with $(Cu_2Se_2)^{2-}$ layers normal to the *c*-axis, depicted in Fig. 2a. The Cu^+ cation site has D_{2d} symmetry, with Cu coordinated by Se^{2-} anions forming distorted $CuSe_4$ tetrahedra. The tetrahedra are compressed in the *ab* plane and elongated along the *c*-axis relative to the perfect tetrahedral environment. The two Se–Cu–Se angles are 102.6(1)° and 113.01(5)°, as shown in Fig. 2b. The Cu–Se bond distance is 2.511(2) Å. The Bi^{3+} ion is coordinated by four O^{2-} and four Se^{2-} anions, forming a distorted square antiprism around the central Bi, as in Fig. 2c. The Cu–Se bond distance 2.518(1) Å in EuCuOSe crystals at room temperature [1] is similar to that found in BiCuOSe. The lattice parameters for BiCuOSe measured in this work at 173 K are smaller than those measured at room temperature [3] by many standard deviations. This is to be expected if the thermal expansion is normal and would imply reasonable thermal expansion coefficients for the *a* and *c* lattice parameters (19 ppm/K and 12 ppm/K, respectively).

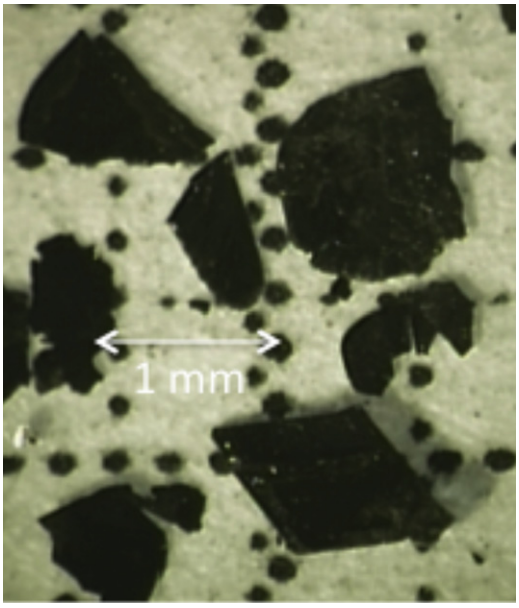

Fig. 1. Optical microscope image of BiCuOSe crystals on mm graph paper.

Table 3
Bond lengths in BiCuOSe and EuCuOSe.

	BiCuOSe[a] (Å)	BiCuOSe[b] (Å)		EuCuOSe[c] (Å)
Bi–O	2.3250(6)	2.33	Eu–O	2.283(1)
Bi–Bi	3.9193(4)		Eu–Eu	3.619(1)
Bi–Se	3.219(2)	3.23	Eu–Se	3.227(1)
Cu–Se	2.511(2)	2.51	Cu–Se	2.518(1)
Cu–Cu	2.7714(3)		Cu–Cu	2.784(1)
Cu–Bi	3.758(1)		Cu–Eu	3.759(1)

[a] Single crystal, −100 °C (this work).
[b] Powder, 25.1 °C [3].
[c] Single crystal, 22 °C [1].

Table 4
Cation-centered bond angles in BiCuOSe.

Bond angles	Angle (deg.)
O(1)#1–Bi(1)–O(1)	73.17(2)
O(1)#1–Bi(1)–O(1)#2	114.88(4)
O(1)#1–Bi(1)–Se(1)#4	141.89(1)
O(1)#2–Bi(1)–Se(1)#4	76.14(4)
Se(1)#4–Bi(1)–Se(1)	118.87(9)
Se(1)#4–Bi(1)–Se(1)#3	75.01(4)
Se(1)–Cu(1)–Se(1)#6	113.01(5)
Se(1)–Cu(1)–Se(1)#5	102.6(1)
Se(1)–Cu(1)–Cu(1)#7	56.50(3)
Se(1)#6–Cu(1)–Cu(1)#7	123.50(3)
Cu(1)#7–Cu(1)–Cu(1)#1	180.00
Cu(1)#7–Cu(1)–Cu(1)#6	90.00

All angles in degrees.
Symmetry transformations used to generate equivalent atoms: #1 $-x, -y, -z$; #2 $-x, -y+1, -z$; #3 $x+1, y, z$; #4 $x+1, y+1, z$; #5 $x, y+1, z$; #6 $-x, -y, -z+1$; #7 $-x-1, -y, -z+1$.

The Bi–O and Bi–Se bond lengths in BiCuOSe are within 1.5% of those in Bi_2O_2Se, where Bi has a similar coordination environment [11]. The Bi–Se bond in BiCuOSe (3.219 Å) is about 6% longer than either of the Bi–Se bonds in Bi_2Se_3 (2.8509 and 3.0748 Å)[17], and the Bi–O length of 2.325 Å is likewise outside of the 2.133–2.229 Å range of Bi–O bond lengths in Bi_2O_3 [18]. The

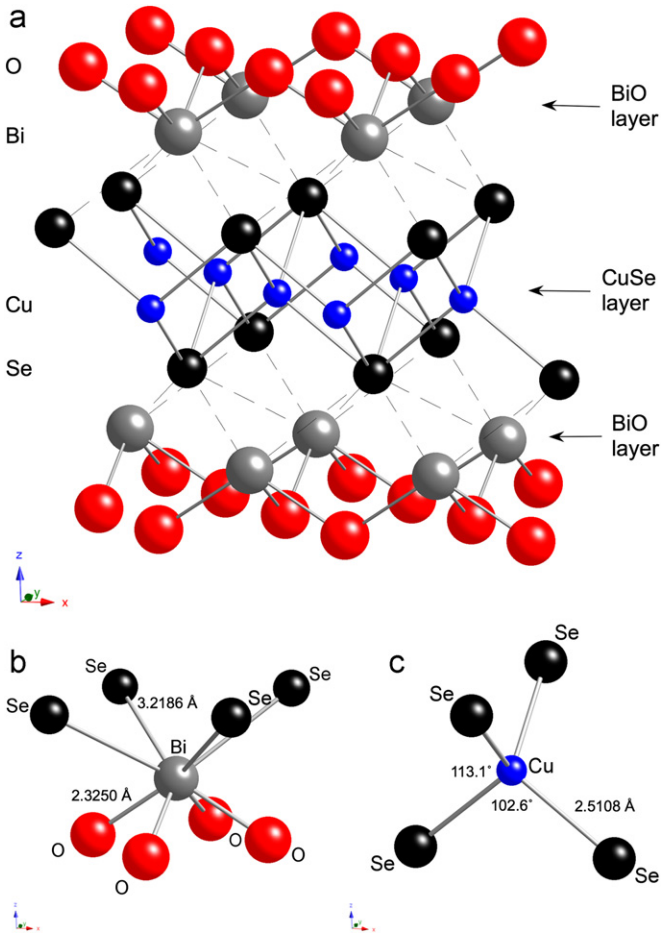

Fig. 2. (a) Structure of BiCuOSe and coordination of (b) Cu and (c) Bi in BiCuOSe.

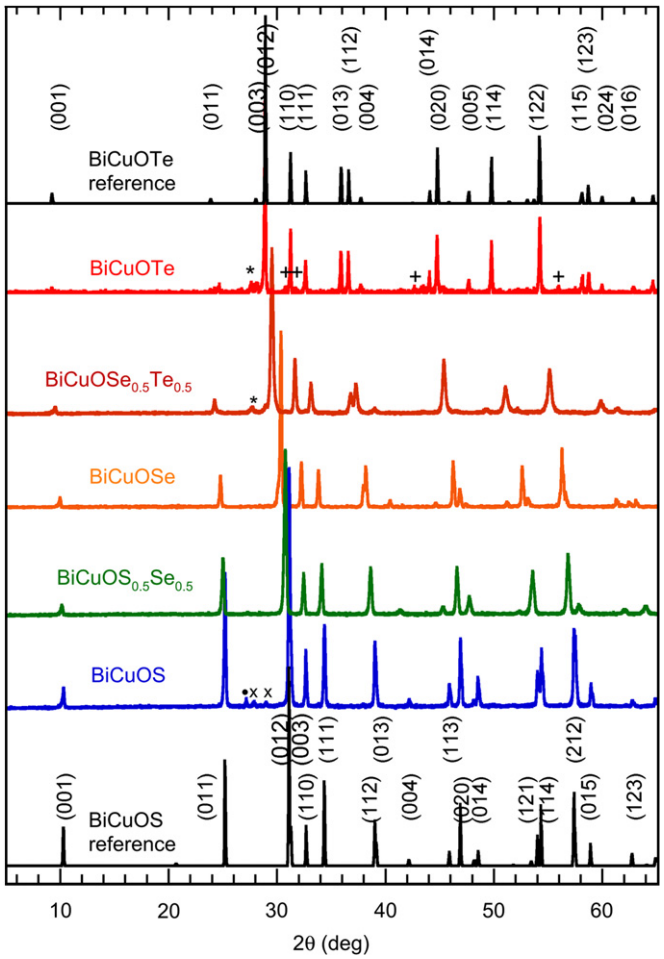

Fig. 3. XRD powder pattern of (bottom to top) BiCuOS, $BiCuOS_{0.5}Se_{0.5}$, BiCuOSe, $BiCuOSe0_{0.5}Te_{0.5}$, and BiCuOTe. Trace secondary phases are marked with * (Bi_2Te_3), • (Bi), x (Cu_3BiS_3),+ (Bi_2O_2Te).

Cu–Se bond (2.511 Å) in BiCuOSe is about 3% longer than the Cu–Se bond (2.445 Å) in the solar cell absorber $CuInSe_2$, which also features monovalent Cu tetrahedrally coordinated by Se [19]. The Cu–Cu bond distance of 2.7714 Å is considerably longer than the Cu–Cu spacing of 2.555 Å in the metal, but shorter than the 3.2187–3.2722 Å range found in the various polymorphs of the delafossite $CuScO_2$ [20], which, like BiCuOSe, is a *p*-type conductor with moderate conductivity and mobility.

The XRD patterns of the solid solution series $BiCuOS_{1-x}Se_x$ (x=0, 0.5, 1) and $BiCuOSe_xTe_{1-x}$ (x=0, 0.5, 1) are graphed in Fig. 3. The shifts of the peaks to lower 2θ values as the larger chalcogenide anion is substituted are nicely evident. The XRD patterns of BiCuOS and BiCuOSe were matched to JCPDS files 46-0436 (BiCuOS) [21] and 45-0296 (BiCuOSe) [6] using the Jade software suite [22], and ICSD 159475 (BiCuOTe) [3]. There are small impurity peaks of Bi and Cu_3BiS_3 in the BiCuOS powder and of Bi_2Te_3 and unreacted Bi_2O_2Te in BiCuOTe, which are indicated in the figure. Features of the XRD patterns of the solid solution series are the decrease in intensities of the (001) and (011) peaks near 2θ=10° and 2θ=25°, respectively, with increasing size of the *Ch*-anion and the emergence of the (103) peak on the low 2θ side of the (112) peak (near 2θ=37°) at the $BiCuOSe_{0.5}Te_{0.5}$ composition. Although the BiCuOTe made via Eq. (2) contained impurities, the method may well represent a viable approach for phase pure powder production. Further refinement of the telluride precursors procedure may be needed to form stoichiometric BiCuOTe powder.

The lattice parameters of $BiCuOCh_{1-x}Ch'_x$ calculated from the positions of the diffraction peaks are plotted in Fig. 4, with statistical error smaller than the point sizes. The data are consistent with solid solubility of the chalcogenide across the entire series, as evidenced by the nearly linear variation in cell parameter with composition. The increase in the *c*/*a* ratio indicates that the distortion of the $CuCh_4$ tetrahedra becomes more pronounced for the larger *Ch* anions, a trend, which is also observed in [3] in the BiCuO*Ch* and LaCuO*Ch* families.

Fig. 5. shows the optical absorption spectra of BiCuOS, $BiCuOS_{0.5}Se_{0.5}$, and BiCuOSe determined from diffuse-reflection measurements. The corresponding band gaps were 1.07, 0.89, and 0.82 eV, displayed in the inset to Fig. 5, which are consistent with the values reported by Stempler et al. [8] and Hiramatsu et al. [3]. The error bars represent variations between samples and between different instruments. These errors are of order 0.1 eV, which illustrates good reproducibility. The decrease in the band gap from BiCuOS to $BiCuOS_{0.5}Se_{0.5}$ to BiCuOSe is clearly evident, but more data are needed to quantify any deviation from linearity. Optical bowing, commonly modeled as a parabolic variation in the band gap with solid solution composition [23,24], has its origins in volume deformation effects and chemical charge transfer [25].

The absorption spectrum of the BiCuOSe single crystal obtained from optical transmission is superimposed on the powder absorption spectrum in Fig. 5. Three crystals of similar thickness were measured to verify the reproducibility of the measurement. There is good agreement between the powder and crystal measurements.

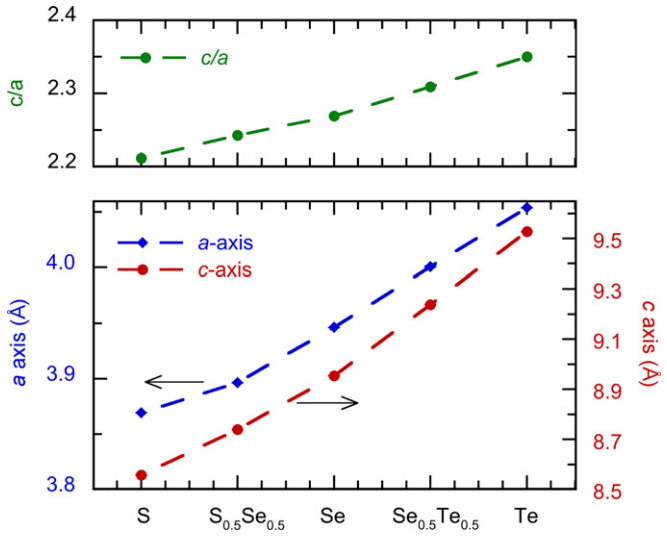

Fig. 4. Unit cell dimensions a and c (bottom) and the c/a ratio (top) for the BiCuO($ChCh'$) solid solutions.

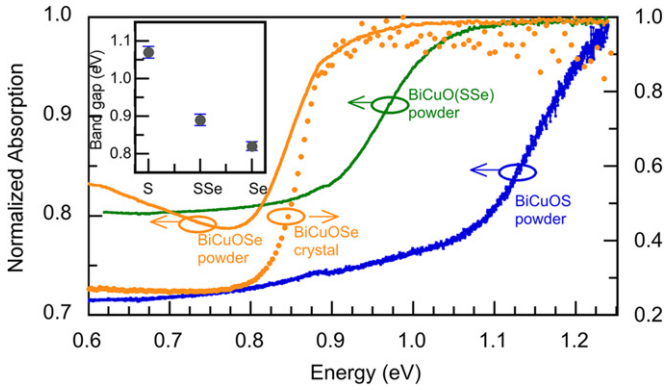

Fig. 5. IR absorption of BiCuOCh powders from diffuse reflection (lines, left scale) and polished BiCuOSe single crystal from transmission (points, right scale). Spectra are normalized to the maximum absorption. Inset: band gap as a function of composition.

The solid solution synthesis described by Eq. (2), and Eqs. (4)–(9), gives a straightforward method to form the compositions $BiCuOS_{0.5}Se_{0.5}$ and $BiCuOSe_{0.5}Te_{0.5}$, but it is not easily generalized to other compositions $BiCuOS_{1-x}Se_x$ or $BiCuOSe_{1-x}Te_x$ except $x=0$, 1. We made BiCuOSe and BiCuOTe by this method, but not BiCuOS. The difficulty lies in the special equipment needed for hydrothermal synthesis of the Bi_2O_2S [26,27] precursor.

4. Conclusion

Crystals of BiCuOSe were made using a flux method and their optical properties were measured. Structural data from single crystal diffraction confirms that BiCuOSe crystallized in the LaCuOCh layered structure; bond lengths and bond angles are in good agreement with published data derived from powder X-ray diffraction. The band gap of the BiCuOSe crystal obtained directly from transmission measurements is 0.82 eV, which is in good agreement with our value derived from diffuse reflection from BiCuOSe powders. Members of the BiCuOCh family can also be prepared by reacting Bi_2O_2Ch and Cu_2Ch powders. Using this method, the mixed compositions $BiCuOS_{0.5}Se_{0.5}$ and $BiCuOSe_{0.5}Te_{0.5}$ and the end members BiCuOSe and BiCuOTe were made. Evidence of the successful formation of the solid solutions comes from XRD, which indicates a smooth variation of the lattice parameters with chalcogenide composition, and also from optical band gap measurements, where the band gap of $BiCuOS_{0.5}Se_{0.5}$ (0.93 eV) lies between that of BiCuOS (1.07 eV) and BiCuOSe (0.82 eV).

Acknowledgments

We thank R. McCann and T. Carvajal, Purdue University; B. McGrath and J. Genco at HemCon, Portland, OR; A. Fasasi and P. R. Griffiths, University of Idaho; E. Espinoza, U.S. Fish and Wildlife Forensic Laboratory for FTIR measurements. Funding was provided by the National Science Foundation under DMR-0804916.

Appendix A. Supporting information

Supplementary data associated with this article can be found in the online version at doi:10.1016/j.jssc.2011.11.013.

References

[1] J. Llanos, R. Cortés, V. Sánchez, Mater. Res. Bull. 43 (2008) 320–325.
[2] Y. Nakachi, K. Ueda, J. Cryst. Growth 311 (2008) 114–117.
[3] H. Hiramatsu, T. Kamiya, H. Yanagi, K. Ueda, M. Hirano, H. Hosono, Chem. Mater. 20 (2007) 326–334.
[4] C.-H. Park, S.-H. Sohn, W.-J. Kwon, S.-T. Hong, T.-H. Kim, United States Patent Application US20110017935, 2011.
[5] A. Ubaldini, E. Giannini, C. Senatore, D. van der Marel, Phys. C 470 (2010) S356–S357.
[6] P.S. Berdonosov, A.M. Kusainova, L.N. Kholodkovskaya, V.A. Dolgikh, L.G. Akselrud, B.A. Popovkin, J. Solid State Chem. 118 (1995) 74–77.
[7] W.C. Sheets, E.S. Stampler, H. Kabbour, M.I. Bertoni, L. Cario, T.O. Mason, T.J. Marks, K.R. Poeppelmeier, Inorg. Chem. 46 (2007) 10741–10748.
[8] E.S. Stampler, W.C. Sheets, M.I. Bertoni, W. Prellier, T.O. Mason, K.R. Poeppelmeier, Inorg. Chem. 47 (2008) 10009–10016.
[9] A. Zakutayev, P. Newhouse, R. Kykyneshi, P.A. Hersh, D.A. Keszler, J. Tate, Appl. Phys. A: Mater. Sci. Process. 102 (2011) 485–492.
[10] T. Mizota, A. Inoue, T. Yamada, A. Nakatsuka, N. Nakayama, Mineral. J 20 (1998) 81–90.
[11] P. Schmidt, O. Rademacher, H. Oppermann, S. Däbritz, Z. Anorg. Allg. Chem. 626 (2000) 1999–2003.
[12] Bruker, SMART, SAINT and SHELXTL, Bruker AXS Inc., Madison, Wisconsin, USA, 2000.
[13] G.M. Sheldrick, SADABS, University of Göttingen, Germany, 1995.
[14] B.H. Toby, J. Appl. Cryst. 34 (2001) 210–213;
A.C. Larson, R.B. Von Dreele, General Structure Analysis System (GSAS), Los Alamos National Laboratory Report LAUR 86-748, 2004;.
[15] A.A. Christy, O.M. Kvalheim, R.A. Velapoldi, Vib. Spectrosc. 9 (1995) 19–27.
[16] P.D. Fochs, Proc. Phys. Soc. B 69 (1956) 70–75.
[17] S. Nakajima, J. Phys. Chem. Solids 24 (1963) 479–485.
[18] H.A. Harwig, Z. Anorg. Allg. Chem. 444 (1978) 151–166.
[19] M.Kh. Rabadanov, I.A. Verin, Inorg. Mater. 34 (1998) 14–16.
[20] J. Li, A.F.T. Yokochi, A.W. Sleight, Solid State Sci. 6 (2004) 831–839.
[21] A.M. Kusainova, P.S. Berdonosov, L.G. Akselrud, L.N. Kholodkovskaya, V.A. Dolgikh, B.A. Popovkin, J. Solid State Chem. 112 (1994) 189–191.
[22] Jade, 8.0, Materials Data, Inc.; Livermore, CA, 2009.
[23] J.E. Bernard, A. Zunger, Phys. Rev. B 34 (1986) 5992–5995.
[24] A. Zunger, J.E. Jaffe, Phys. Rev. Lett. 51 (1983) 662–665.
[25] A. Zaoui, J. Phys.: Condens. Matter 14 (2002) 4025–4033.
[26] H. Hsu, Part 1. The Synthesis and Properties Characterization of Bi_2O_2S; Part 2. Identification of the 90 K High Tc Superconductor and its Phase Relationship with $La_3Ba_3Cu_6O_{14+y}$, Master's Thesis, University of Texas at Austin, 1988.
[27] E. Koyama, I. Nakai, K. Nagashima, Acta Crystallogr. B: Struct. Sci. 40 (1984) 105–109.